Computational Geometry 47 (2014) 15–24

Contents lists available at ScienceDirect

Computational Geometry: Theory and Applications

www.elsevier.com/locate/comgeo

Overlap of convex polytopes under rigid motion ☆

Hee-Kap Ahn [a], Siu-Wing Cheng [b,*], Hyuk Jun Kweon [a], Juyoung Yon [b]

[a] Department of Computer Science and Engineering, POSTECH, Republic of Korea
[b] Department of Computer Science and Engineering, HKUST, Hong Kong

ARTICLE INFO

Article history:
Received 3 December 2012
Accepted 1 August 2013
Available online 7 August 2013
Communicated by M. de Berg

Keywords:
Convex polyhedron
Shape matching
Rigid motion
Overlap
Approximation algorithm

ABSTRACT

We present an algorithm to compute a rigid motion that approximately maximizes the volume of the intersection of two convex polytopes P_1 and P_2 in $\mathbb{R}^3$. For all $\varepsilon \in (0, 1/2]$ and for all $n \geqslant 1/\varepsilon$, our algorithm runs in $O(\varepsilon^{-3} n \log^{3.5} n)$ time with probability $1 - n^{-O(1)}$. The volume of the intersection guaranteed by the output rigid motion is a $(1-\varepsilon)$-approximation of the optimum, provided that the optimum is at least $\lambda \cdot \max\{|P_1|, |P_2|\}$ for some given constant $\lambda \in (0, 1]$.

1. Introduction

Shape matching is a common task in many object recognition problems. A translation or rigid motion of one shape is sought that maximizes some similarity measure with another shape. Convex shape matching algorithms have been used in tracking regions in an image sequence [10] and measuring symmetry of a convex body [8]. We define the *overlap* of two convex shapes to be the volume of their intersection, which is a robust similarity measure [12]. In this paper, we consider the problem of finding the maximum overlap of two convex polytopes in $\mathbb{R}^3$ under rigid motion.

Efficient algorithms have been developed for two convex n-gons in the plane. De Berg et al. [5] developed an algorithm to find the maximum overlap of two convex polygons under translation in $O(n \log n)$ time. Ahn et al. [4] presented two algorithms to find a $(1-\varepsilon)$-approximate maximum overlap, one for the translation case and another for the rigid motion case. They assume that the polygon vertices are stored in arrays in clockwise order around the polygon boundaries. Ahn et al.'s algorithms run in $O(\varepsilon^{-1} \log n + \varepsilon^{-1} \log(1/\varepsilon))$ time for the translation case and $O(\varepsilon^{-1} \log n + \varepsilon^{-2} \log(1/\varepsilon))$ time for the rigid motion case. Cheong et al. [7] gave an algorithm to align two simple polygons P_1 and P_2 by a rigid motion so that their overlap is at least the optimum minus $\varepsilon \cdot \min\{|P_1|, |P_2|\}$. The running time is $O((n^3/\varepsilon^8) \log^5 n)$. Cheng and Lam [6] recently improved the running time to $O((n^3/\varepsilon^4) \log^{5/3} n \log^{5/3} \frac{n}{\varepsilon})$. Finding the exact maximum overlap under rigid motion seems difficult. A brute force approach is to subdivide the space of rigid motion $(-\pi, \pi] \times \mathbb{R}^2$ into cells so that the intersecting pairs of polygon edges do not change within a cell. The hope is to obtain a formula for the maximum overlap within a cell as the intersection does not change combinatorially, and then compute the maximum of the formula. Unfortunately, the subdivision of $(-\pi, \pi] \times \mathbb{R}^2$ has curved edges and facets. Also the formula is a sum of a large number

☆ Research of Cheng and Yon was partly supported by the Research Grant Council, Hong Kong, China, project no. 611711. Research of Yon was also supported by the Hong Kong PhD Fellowship. Research by Ahn was partly supported by the NRF grant 2011-0030044 (SRC-GAIA) funded by the government of Korea.

* Corresponding author.
E-mail addresses: heekap@postech.ac.kr (H.-K. Ahn), scheng@cse.ust.hk (S.-W. Cheng), kweon7182@postech.ac.kr (H.J. Kweon), jyon@cse.ust.hk (J. Yon).

0925-7721/$ – see front matter
http://dx.doi.org/10.1016/j.comgeo.2013.08.001

of fractions, and optimizing the formula seems to require solving a high-degree polynomial system. These issues make it a challenge to optimize the formula in a cell.

Fewer algorithmic results are known concerning the maximum overlap of two convex polytopes in $\mathbb{R}^d$ for $d \geqslant 3$. Let n be the number of hyperplanes defining the convex polytopes. Ahn et al. [2] developed an algorithm to find the maximum overlap of two convex polytopes under translation in $O(n^{(d+1-3/d)\lfloor d/2 \rfloor} \log^{d+1} n)$ expected time. Recently, Ahn, Cheng and Reinbacher [3] have obtained substantially faster algorithms to align two convex polytopes under translation in $\mathbb{R}^d$ for $d \geqslant 3$. The overlap computed is no less than the optimum minus μ, where μ is any small constant fixed in advance. The running times are $O(n \log^{3.5} n)$ for $\mathbb{R}^3$ and $O(n^{\lfloor d/2 \rfloor + 1} \log^d n)$ for $d \geqslant 4$, and these time bounds hold with probability $1 - n^{-O(1)}$. There is no specific prior result concerning the maximum overlap of convex polytopes under rigid motion. Vigneron [13] studied the optimization of algebraic functions and one of the applications is the alignment of two possibly non-convex polytopes under rigid motion. For any $\varepsilon \in (0, 1)$ and any two convex polytopes with n defining hyperplanes, Vigneron's method can return in $O(\varepsilon^{-\Theta(d^2)} n^{\Theta(d^3)} (\log \frac{n}{\varepsilon})^{\Theta(d^2)})$ time an overlap under rigid motion that is at least $1 - \varepsilon$ times the optimum. Finding the exact overlap is even more challenging in $\mathbb{R}^3$.

In this paper, we present a new algorithm to approximate the maximum overlap of two convex polytopes P_1 and P_2 in $\mathbb{R}^3$ under rigid motion. For the purpose of shape matching, it often suffices to know that two input shapes are very dissimilar if this is the case. Therefore, we are only interested in matching P_1 and P_2 when their maximum overlap under rigid motion is at least $\lambda \cdot \max\{|P_1|, |P_2|\}$ for some given constant $\lambda \in (0, 1]$, where $|P_i|$ denotes the volume of P_i. Under this assumption, for all $\varepsilon \in (0, 1/2]$ and for all $n \geqslant 1/\varepsilon$, our algorithm runs in $O(\varepsilon^{-3} n \log^{3.5} n)$ time with probability $1 - n^{-O(1)}$ and returns a rigid motion that achieves a $(1-\varepsilon)$-approximate maximum overlap. The assumption can be verified as follows. Run our algorithm using $\lambda/2$ instead of λ. Check if the overlap output by our algorithm is at least $(1 - \varepsilon)\lambda \cdot \max\{|P_1|, |P_2|\}$. If not, we know that the assumption is not satisfied. If yes, the maximum overlap is at least $(\lambda/2) \cdot \max\{|P_1|, |P_2|\}$ and our algorithm's output is a $(1 - \varepsilon)$-approximation because we used $\lambda/2$ in running the algorithm. Our high-level strategy has two steps. First, sample a set of rotations. Second, for each sampled rotation, apply it and then apply the almost optimal translation computed by Ahn et al.'s algorithm [3]. Finally, return the best answer among all rigid motions tried.

If one uses a very fine uniform discretization of the rotation space, it is conceptually not difficult to sample rotations so that the resulting approximation is good. The problem is that such a discretization inevitably leads to a running time that depends on some geometric parameters of P_1 and P_2. In order to obtain a running time that depends on n and ε only, we cannot use a uniform discretization of the entire rotation space. Indeed, our contribution lies in establishing some structural properties that allow us to discretize a small subset of the rotation space, and exploiting this discretization in the analysis to prove the desired approximation. This approach is also taken in the 2D case in [4], but our analysis is not an extension of that in [4] as the three-dimensional situation is very different.

2. Similar polytopes

In this section, we show that P_1 and P_2 are "similar" under the assumption that their maximum overlap is at least $\lambda \cdot \max\{|P_1|, |P_2|\}$. We use the Löwner–John ellipsoid [11] to identify three axes of P_1 and P_2. For every convex body P in $\mathbb{R}^d$, it is proven by Löwner that there is a unique smallest ellipsoid E that contains P. Then John proved that $\frac{1}{d}E$ is contained in P. There are various algorithms for finding an ellipsoid of this flavor.

Lemma 1. *(See [11].) Let P be a convex body with m vertices in $\mathbb{R}^3$. For every $\eta > 0$, an ellipsoid $\mathcal{E}(P)$ can be computed in $O(m/\eta)$ time such that $\frac{1}{3(1+\eta)}\mathcal{E}(P) \subset P \subset \mathcal{E}(P)$.*

For $i \in \{1, 2\}$, we use $\mathcal{E}(P_i)$ to denote the ellipsoid guaranteed by Lemma 1 for P_i, using the setting of $\eta = 1/3$. There are three mutually orthogonal directed lines α_i, β_i and γ_i through the center of $\mathcal{E}(P_i)$ such that $|\alpha_i \cap \mathcal{E}(P_i)|$ and $|\gamma_i \cap \mathcal{E}(P_i)|$ are the shortest and longest, respectively, among all possible directed lines through the center of $\mathcal{E}(P_i)$. After fixing α_i and γ_i, there are two choices for β_i and any one will do. We call these directed lines the α_i-, β_i-, and γ_i-axes of P_i. The lengths $a_i = |\alpha_i \cap \mathcal{E}(P_i)|$, $b_i = |\beta_i \cap \mathcal{E}(P_i)|$, and $c_i = |\gamma_i \cap \mathcal{E}(P_i)|$ are the three *principal diameters* of $\mathcal{E}(P_i)$. Notice that $a_i \leqslant b_i \leqslant c_i$. Define $a_{\min} = \min\{a_1, a_2\}$, $b_{\min} = \min\{b_1, b_2\}$, and $c_{\min} = \min\{c_1, c_2\}$. The following result gives an upper bound on the maximum overlap of P_1 and P_2.

Lemma 2. *For $i \in \{1, 2\}$, let R_i be a box with side lengths a_i, b_i, and c_i. The maximum overlap of R_1 and R_2 under rigid motion is at most $\sqrt{2} a_{\min} b_{\min} c_{\min}$.*

Proof. Without loss of generality, we suppose that a_1 is $a_{\min}$, that is, $a_1 \leqslant a_2$. If $b_{\min} = b_1$ and $c_{\min} = c_1$, then the maximum overlap of R_1 and R_2 under rigid motion is $|R_1| = a_{\min} b_{\min} c_{\min}$. There are three cases left: (1) $b_{\min} = b_2$ and $c_{\min} = c_2$, (2) $b_{\min} = b_1$ and $c_{\min} = c_2$, and (3) $b_{\min} = b_2$ and $c_{\min} = c_1$. For $i \in \{1, 2\}$, let the ab-plane of R_i be the plane through the center of R_i and parallel to the facets of side lengths a_i and b_i. The bc-plane and ac-plane of R_i are defined analogously. Let L_i^{ab} be the line through the center of R_i and perpendicular to the ab-plane of R_i. The lines L_i^{bc} and L_i^{ac} are defined analogously. In the rest of the proof, assume that R_1 and R_2 have been placed such that their overlap is maximum.

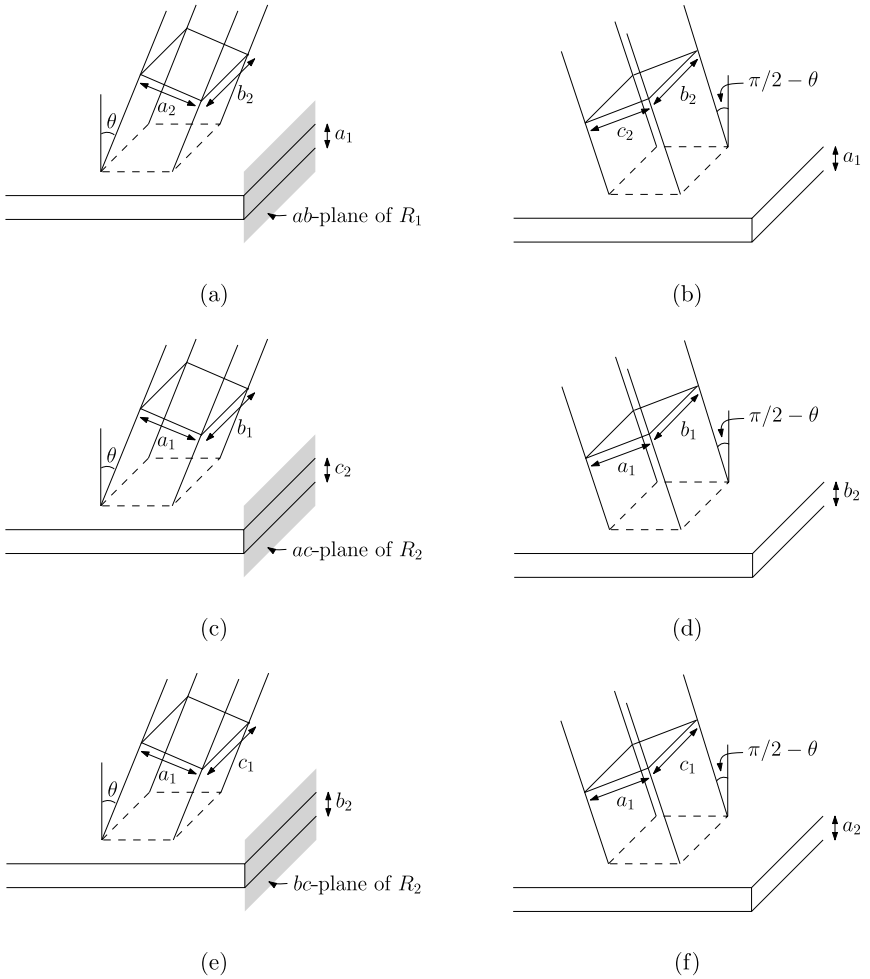

Fig. 1. Illustrations for the proof of Lemma 2.

Case 1. $b_{\min} = b_2$ and $c_{\min} = c_2$. Let θ be the nonobtuse angle between L_1^{bc} and L_2^{ab}. Suppose that $\theta \leqslant \pi/4$. Refer to Fig. 1(a). Consider the two facets of R_1 that are parallel to its bc-plane. The supporting planes of these two facets bound an infinite slab with thickness a_1. Consider the facets of R_2 that are parallel to its ab-plane. Sweeping these two facets along L_2^{ab} produces an infinite rectangular cylinder. The intersection of the slab and the cylinder is a parallelepiped that contains $R_1 \cap R_2$, so it suffices to bound the volume of this parallelepiped. We rotate the cylinder around L_2^{ab} so that its facets with width b_2 make an angle θ with the ab-plane of R_1. Note that the volume of the parallelepiped is not changed by this rotation. The parallelepiped's volume is $a_1a_2b_2/\cos\theta \leqslant a_1b_2c_2/\cos\theta \leqslant \sqrt{2}a_{\min}b_{\min}c_{\min}$. Suppose that $\theta > \pi/4$. Refer to Fig. 1(b). The angle between L_1^{bc} and L_2^{bc} is $\pi/2 - \theta$. We keep the same infinite slab as in the above. We sweep the two facets of R_2 that are parallel to its bc-plane along L_2^{bc} to obtain an infinite rectangular cylinder. The volume of the parallelepiped at the intersection of the slab and this new cylinder is $a_1b_2c_2/\cos(\pi/2 - \theta) \leqslant \sqrt{2}a_{\min}b_{\min}c_{\min}$.

Case 2. $b_{\min} = b_1$ and $c_{\min} = c_2$. Let θ be the nonobtuse angle between L_1^{ab} and L_2^{ab}. Suppose that $\theta \leqslant \pi/4$. Refer to Fig. 1(c). Consider the two facets of R_2 that are parallel to its ab-plane. The supporting planes of these two facets bound an infinite slab with thickness c_2. Consider the facets of R_1 that are parallel to its ab-plane. Sweeping these two facets along L_1^{ab} produces an infinite rectangular cylinder. As in case 1, we rotate the cylinder around L_1^{ab} so that its facets with width b_1 make an angle θ with the ac-plane of R_2. The intersection of the slab and the cylinder is a parallelepiped that contains $R_1 \cap R_2$, and the parallelepiped's volume is $a_1b_1c_2/\cos\theta \leqslant \sqrt{2}a_{\min}b_{\min}c_{\min}$. Suppose that $\theta > \pi/4$. Refer to Fig. 1(d). The angle between L_1^{ab} and L_2^{ac} is $\pi/2 - \theta < \pi/4$. We replace the slab by the slab bounded above by facets of R_2 that are parallel to its ac-plane. $R_1 \cap R_2$ is contained in the parallelepiped at the intersection of the new slab and the cylinder, whose volume is at most $a_1b_1b_2/\cos(\pi/2 - \theta) \leqslant a_1b_1c_2/cos(\pi/2 - \theta) \leqslant \sqrt{2}a_{\min}b_{\min}c_{\min}$.

Case 3. $b_{\min} = b_2$ and $c_{\min} = c_1$. Let θ be the nonobtuse angle between L_1^{ac} and L_2^{ac}. Sweep the facets of R_1 that are parallel to its ac-plane along L_1^{ac} to obtain an infinite cylinder. We rotate the cylinder around L_1^{ac} so that its facets with width c_1

make an angle θ with the bc-plane of R_2. If $\theta \leqslant \pi/4$, take the slab bounded by the facets of R_2 that are parallel to its ac-plane. Refer to Fig. 1(e). If $\theta > \pi/4$, take the slab bounded by the facets of R_2 that are parallel to its bc-plane. Refer to Fig. 1(f). Then, we can argue as in case 2 that $|R_1 \cap R_2| \leqslant \sqrt{2}a_{\min}b_{\min}c_{\min}$. □

We are ready to show that P_1 and P_2 are similar in the sense that the respective principal diameters are within a constant factor of each other.

Lemma 3. *If the maximum overlap of P_1 and P_2 under rigid motion is $\lambda \cdot \max\{|P_1|, |P_2|\}$ or more, then the ratios a_1/a_2, b_1/b_2, and c_1/c_2 are between $\lambda/(2^7\sqrt{2})$ and $2^7\sqrt{2}/\lambda$.*

Proof. It follows from Lemma 1 that for $i \in \{1,2\}$, $|P_i| \geqslant \frac{4}{3}\pi \cdot 2^{-3}3^{-3}(1+\eta)^{-3} \cdot a_ib_ic_i$. Since we set $\eta = 1/3$ to compute $\mathcal{E}(P_i)$, we obtain $|P_i| \geqslant \frac{4}{3}\pi \cdot 2^{-3}4^{-3} \cdot a_ib_ic_i$. The maximum overlap of P_1 and P_2 under rigid motion is at most $\sqrt{2}a_{\min}b_{\min}c_{\min}$ by Lemma 2. Thus, $\sqrt{2}a_{\min}b_{\min}c_{\min} \geqslant \lambda|P_i| \geqslant (3/\pi) \cdot \lambda|P_i| \geqslant \lambda a_ib_ic_i/2^7$. It follows that

$$a_1/a_2 \leqslant \left(2^7\sqrt{2}/\lambda\right) \cdot (b_{\min}/b_1) \cdot (c_{\min}/c_1) \leqslant 2^7\sqrt{2}/\lambda$$
$$a_1/a_2 \geqslant \left(\lambda/\left(2^7\sqrt{2}\right)\right) \cdot (b_2/b_{\min}) \cdot (c_2/c_{\min}) \geqslant \lambda/\left(2^7\sqrt{2}\right)$$

We can similarly show that the ratios b_1/b_2 and c_1/c_2 are between $\lambda/(2^7\sqrt{2})$ and $2^7\sqrt{2}/\lambda$. □

3. Sampling rigid motions

A rigid motion can be viewed as a rotation of P_1 and P_2 followed by a translation of P_2. A rotation is a relative motion between P_1 and P_2, and indeed, it is more convenient to rotate both P_1 and P_2 for our purposes. We set the initial positions of P_1 and P_2 so that the centers of $\mathcal{E}(P_1)$ and $\mathcal{E}(P_2)$ coincide and the α_1- and α_2-axes, β_1- and β_2-axes, and the γ_1- and γ_2-axes are aligned, respectively.

A rotation R_* is decomposed into three simpler rotations R_β, R_α, and R_γ parametrized by three angles $\theta_\beta, \theta_\alpha, \theta_\gamma \in (-\pi, \pi]$, respectively, such that $R_\gamma(R_\beta(P_1))$ is the image of P_1 under R_* and $R_\alpha(P_2)$ is the image of P_2 under R_*. The detailed specification of R_* is as follows. Let $\angle(u, v)$ denote the angle between two oriented axes u and v.

1. Rotate P_1 around the β_1-axis clockwise by the angle θ_β as viewed from infinity in β_1's direction. This is the rotation R_β which fixes the angle $\angle(R_\beta(\gamma_1), \alpha_2)$.
2. Rotate P_2 around the α_2-axis clockwise by the angle θ_α as viewed from infinity in α_2's direction. This is the rotation R_α which fixes the angle $\angle(R_\beta(\gamma_1), R_\alpha(\beta_2))$. Note that $\angle(R_\beta(\gamma_1), R_\alpha(\alpha_2)) = \angle(R_\beta(\gamma_1), \alpha_2)$, i.e., R_α does not affect $\angle(R_\beta(\gamma_1), \alpha_2)$.
3. Rotate $R_\beta(P_1)$ around $R_\beta(\gamma_1)$ clockwise by the angle θ_γ as viewed from infinity in the direction of $R_\beta(\gamma_1)$. This is the rotation R_γ. Note that $\angle(R_\gamma(R_\beta(\gamma_1)), \alpha_2) = \angle(R_\beta(\gamma_1), \alpha_2)$ and $\angle(R_\gamma(R_\beta(\gamma_1)), R_\alpha(\beta_2)) = \angle(R_\beta(\gamma_1), R_\alpha(\beta_2))$, i.e., R_γ does not affect $\angle(R_\beta(\gamma_1), \alpha_2)$ and $\angle(R_\beta(\gamma_1), R_\alpha(\beta_2))$.

The order of the applications of R_β, R_α and R_γ matters—the result of applying R_β, R_α and R_γ in this order can differ from the result of applying the same three rotations in another order.

The next result restricts the ranges of θ_β, θ_α, and θ_γ that contain the optimal rotation.

Lemma 4. *Let P_1 and P_2 be two convex polytopes in $\mathbb{R}^3$. Let $\mathring{R}_*$ be the rotation part of an optimal rigid motion that maximizes the overlap of P_1 and P_2. Let $\mathring{\theta}_\beta$, $\mathring{\theta}_\alpha$ and $\mathring{\theta}_\gamma$ be the three angles in the representation of $\mathring{R}_*$. If $2^{20}3a_{\min} \leqslant \lambda^2 c_{\min}/\sqrt{2}$, then*

$$|\sin\mathring{\theta}_\beta| \leqslant \frac{2^{20}3a_{\min}}{\lambda^2 c_{\min}}, \qquad |\sin\mathring{\theta}_\alpha| \leqslant \frac{2^{20}3\sqrt{2}b_{\min}}{\lambda^2 c_{\min}}, \qquad |\sin\mathring{\theta}_\gamma| \leqslant \frac{2^{20}3a_{\min}}{\lambda^2 b_{\min}}.$$

Proof. By Lemma 1 and the setting of $\eta = 1/3$, if we position P_1 and P_2 such that the centers of $\mathcal{E}(P_1)$ and $\mathcal{E}(P_2)$ coincide and the respective axes of P_1 and P_2 are aligned, then $P_1 \cap P_2$ contains an ellipsoid with principal diameters $a_{\min}/4$, $b_{\min}/4$, and $c_{\min}/4$. Let $\mathring{T}$ denote the translation part of the optimal rigid motion. Thus, $|\mathring{R}_\gamma(\mathring{R}_\beta(P_1)) \cap \mathring{T}(\mathring{R}_\alpha(P_2))| \geqslant 4\pi a_{\min}b_{\min}c_{\min}/(2^9 3)$.

Enclose $\mathcal{E}(P_1)$ in an infinite elliptic cylinder C such that the base of C has principal diameters a_1 and b_1, and the axis of C is aligned with the γ_1-axis of P_1. Enclose $\mathcal{E}(P_2)$ with an infinite slab S that has thickness a_2 and is parallel to the $\beta_2\gamma_2$-plane. Refer to Fig. 2(a). When we apply $\mathring{R}_*$, we get $|\mathring{R}_\gamma(\mathring{R}_\beta(P_1)) \cap \mathring{R}_\alpha(P_2)| \leqslant |\mathring{R}_\gamma(\mathring{R}_\beta(C)) \cap \mathring{R}_\alpha(S)|$. Only $\mathring{R}_\beta$ has an effect on $|\mathring{R}_\gamma(\mathring{R}_\beta(C)) \cap \mathring{R}_\alpha(S)|$ because $\mathring{R}_\alpha$ does not change the shape of the intersection, and $\mathring{R}_\gamma$ does not change the volume of the intersection as long as $\mathring{\theta}_\beta \notin \{0, \pi\}$. The base area and height of $\mathring{R}_\gamma(\mathring{R}_\beta(C)) \cap \mathring{R}_\alpha(S)$ are $\pi a_1b_1/(2^2|\sin\mathring{\theta}_\beta|)$ and a_2, respectively. Therefore, $|\mathring{R}_\gamma(\mathring{R}_\beta(C)) \cap \mathring{R}_\alpha(S)| = \pi a_1a_2b_1/(2^2|\sin\mathring{\theta}_\beta|)$. Applying the translation $\mathring{T}$ to $\mathring{R}_\alpha(S)$ has no

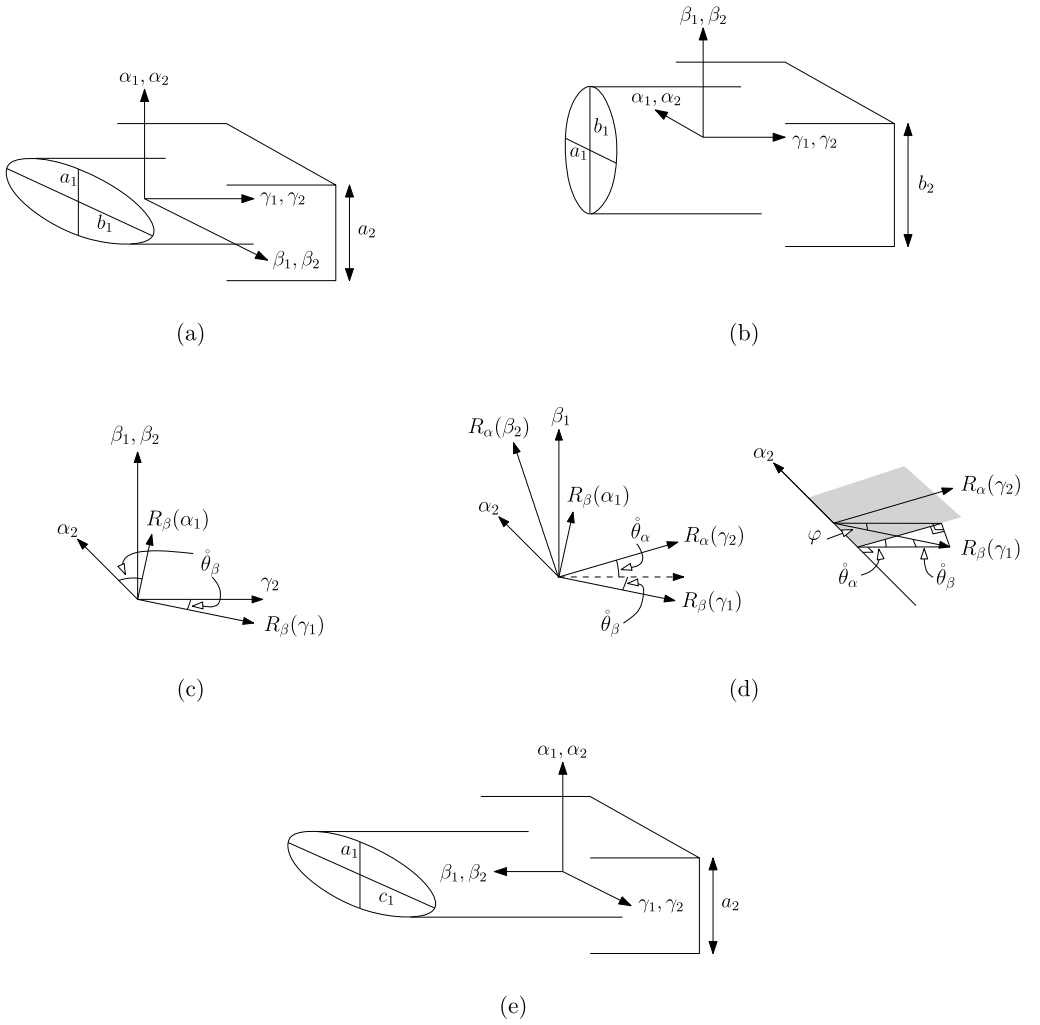

Fig. 2. (a) Bounding $|\sin\mathring{\theta}_\beta|$. (b) Bounding $|\sin\mathring{\theta}_\alpha|$. (c) Effect of R_β. (d) The shaded patch indicates the plane spanned by α_2 and $R_\alpha(\gamma_2)$. R_α makes $R_\beta(\gamma_1)$ tilt at an angle φ to this plane. (e) Bounding $|\sin\mathring{\theta}_\gamma|$.

impact on the intersection volume. Therefore, $|\mathring{R}_\gamma(\mathring{R}_\beta(C)) \cap \mathring{R}_\alpha(S)| \geqslant |\mathring{R}_\gamma(\mathring{R}_\beta(P_1)) \cap \mathring{T}(\mathring{R}_\alpha(P_2))| \geqslant 4\pi a_{\min} b_{\min} c_{\min}/(2^9 3)$. We conclude that

$$\frac{4\pi}{2^9 3} a_{\min} b_{\min} c_{\min} \leqslant \frac{\pi}{2^2 |\sin\mathring{\theta}_\beta|} a_1 a_2 b_1$$

and therefore

$$|\sin\mathring{\theta}_\beta| \leqslant \frac{2^5 3 a_1 a_2 b_1}{a_{\min} b_{\min} c_{\min}} \leqslant \frac{2^{20} 3 a_{\min}}{\lambda^2 c_{\min}}.$$

The last inequality follows from Lemma 3.

The assumption of $2^{20} 3 a_{\min} \leqslant \lambda^2 c_{\min}/\sqrt{2}$ is needed in bounding $|\sin\mathring{\theta}_\alpha|$. This assumption implies that $|\sin\mathring{\theta}_\beta| \leqslant 1/\sqrt{2}$ and, therefore, $\mathring{\theta}_\beta \in (-\pi, -3\pi/4] \cup [-\pi/4, \pi/4] \cup [3\pi/4, \pi]$. To bound $|\sin\mathring{\theta}_\alpha|$, we similarly enclose $\mathcal{E}(P_1)$ with an infinite elliptic cylinder C and $\mathcal{E}(P_2)$ with a slab S, except that we swap the positions of α_i and β_i. The thickness of the slab S enclosing $\mathcal{E}(P_2)$ is thus b_2. Fig. 2(b) gives an illustration. Refer to Fig. 2(c). R_β rotates P_1 around the β_1-axis by the angle $\mathring{\theta}_\beta$ and the angle between α_2 and $R_\beta(\gamma_1)$ will not be changed by R_α. Refer to Fig. 2(d). R_α makes C tilt at a nonobtuse angle φ to S, while R_γ has no effect on the volume of the intersection of C and S as long as $\mathring{\theta}_\alpha \notin \{0, \pi\}$. Note that φ is the nonobtuse angle between $R_\beta(\gamma_1)$ and the plane spanned by α_2 and $R_\alpha(\gamma_2)$. The maximum value of $\sin\varphi$ is $|\sin\mathring{\theta}_\alpha|$ when $\mathring{\theta}_\beta = 0$ or π. The minimum value of $\sin\varphi$ is attained when $\mathring{\theta}_\beta = \pm\pi/4$ or $\pm 3\pi/4$, and by elementary trigonometry, the minimum value of $\sin\varphi$ is $|\sin\mathring{\theta}_\alpha|/\sqrt{2}$. Using an analysis similar to that for $\mathring{\theta}_\beta$, we obtain $|\mathring{R}_\gamma(\mathring{R}_\beta(C)) \cap \mathring{R}_\alpha(S)| = \pi a_1 b_1 b_2/(2^2 \sin\varphi) \leqslant \pi a_1 b_1 b_2/(2\sqrt{2}|\sin\mathring{\theta}_\alpha|)$. Therefore,

$$\frac{4\pi}{2^9 3} a_{\min} b_{\min} c_{\min} \leqslant \frac{\pi}{2\sqrt{2}|\sin\mathring{\theta}_\alpha|} a_1 b_1 b_2$$

and

$$|\sin\mathring{\theta}_\alpha| \leqslant \frac{2^6 3 a_1 b_1 b_2}{\sqrt{2} a_{\min} b_{\min} c_{\min}} \leqslant \frac{2^{20} 3\sqrt{2} b_{\min}}{\lambda^2 c_{\min}}.$$

The analysis for bounding $|\sin\mathring{\theta}_\gamma|$ is similar. We enclose $\mathcal{E}(P_1)$ with an infinite elliptic cylinder C and $\mathcal{E}(P_2)$ with a slab S as shown in Fig. 2(e). The thickness of S is a_2. R_β has no effect on the volume of the intersection of C and S as long as $\mathring{\theta}_\gamma \notin \{0, \pi\}$, and R_α does not change the shape of intersection of C and S. R_γ makes C tilt at an angle $\mathring{\theta}_\gamma$ to S. Therefore, $|\mathring{R}_\gamma(\mathring{R}_\beta(C)) \cap \mathring{R}_\alpha(S)| = \pi a_1 a_2 c_1/(2^2|\sin\mathring{\theta}_\gamma|)$. Therefore,

$$\frac{4\pi}{2^9 3} a_{\min} b_{\min} c_{\min} \leqslant \frac{\pi}{2^2|\sin\mathring{\theta}_\gamma|} a_1 a_2 c_1$$

and

$$|\sin\mathring{\theta}_\gamma| \leqslant \frac{2^5 3 a_1 a_2 c_1}{a_{\min} b_{\min} c_{\min}} \leqslant \frac{2^{20} 3 a_{\min}}{\lambda^2 b_{\min}}. \qquad \square$$

By Lemma 4, if $2^{20}3a_{\min} \leqslant \lambda^2 c_{\min}/\sqrt{2}$, then θ_β, θ_α and θ_γ can only vary in some appropriate subsets of $(-\pi, \pi]$. This allows us to discretize only a small subset of $(-\pi, \pi]$ in designing our approximation algorithm, which helps reducing the running time. If $2^{20}3a_{\min} > \lambda^2 c_{\min}/\sqrt{2}$, the lengths a_i, b_i and c_i are within constant factors of each other, and it suffices to discretize the range $(-\pi, \pi]$ uniformly in this case. In the following, we define the angular ranges I_β, I_α and I_γ for θ_β, θ_α and θ_γ respectively, and then discuss how to discretize these ranges.

- If $2^{20}3a_{\min} > \lambda^2 c_{\min}/\sqrt{2}$, then $I_\beta = I_\alpha = I_\gamma = (-\pi, \pi]$.
- If $2^{20}3a_{\min} \leqslant \lambda^2 c_{\min}/\sqrt{2}$, then for all $\xi \in \{\beta, \alpha, \gamma\}$,

  $$I_\xi = (-\pi, -\pi + f_\xi] \cup [-f_\xi, f_\xi] \cup [\pi - f_\xi, \pi],$$

  where:
  - $f_\beta = \arcsin(2^{20}3a_{\min}/(\lambda^2 c_{\min}))$.
  - $f_\alpha = \arcsin(2^{20}3\sqrt{2}b_{\min}/(\lambda^2 c_{\min}))$ if $2^{20}3\sqrt{2}b_{\min} \leqslant \lambda^2 c_{\min}$; otherwise, $f_\alpha = \pi$.
  - $f_\gamma = \arcsin(2^{20}3a_{\min}/(\lambda^2 b_{\min}))$ if $2^{20}3a_{\min} \leqslant \lambda^2 b_{\min}$; otherwise, $f_\gamma = \pi$.

The rotation part $\mathring{R}_*$ of the optimal rigid motion belongs to $I_\beta \times I_\alpha \times I_\gamma$ according to Lemma 4. We sample angles from I_β, I_α, and I_γ at intervals of $\varepsilon\Delta_\beta$, $\varepsilon\Delta_\alpha$, and $\varepsilon\Delta_\gamma$ respectively, where

$$\Delta_\beta = \frac{a_{\min} b_{\min} c_{\min}}{2 \cdot 3^6 b_1 c_1^2}, \qquad \Delta_\alpha = \frac{a_{\min} b_{\min} c_{\min}}{3^5 a_2 c_2^2}, \qquad \Delta_\gamma = \frac{a_{\min} b_{\min} c_{\min}}{3^5 b_1^2 c_1}.$$

Let S_ξ denote the set of angles sampled from I_ξ for every $\xi \in \{\beta, \alpha, \gamma\}$. Our strategy is to try all rotations in $S_\beta \times S_\alpha \times S_\gamma$ and for each such rotation, find the best translation to maximize the overlap. It remains to show that the best rigid motion obtained by this strategy gives a $(1-\varepsilon)$-approximation.

We first prove a technical lemma about rotating a planar convex set. It is similar to Lemma 4 in [1], except that the rotation center can be outside the convex set.

Lemma 5. *Let C be a convex set in $\mathbb{R}^2$. Let C' be a copy of C rotated by an angle δ around a point p that is at distance l or less from every point in C. Then $|C \backslash C'| \leqslant (\pi\delta l/2) \cdot \mathrm{diam}(C) + \pi\delta^2 l^2/8$.*

Proof. We denote by D the symmetric difference between C and C'. Note that $|D| = |C| - |C \cap C'| + |C'| - |C \cap C'| = 2(|C| - |C \cap C'|) = 2|C \backslash C'|$. Let C'' be a copy of C rotated by an angle $\delta/2$ around p in the same direction as the rotation from C to C'. Let T be the set of points that are at distance $\delta l/2$ or less from the boundary of C''.

If we rotate C'' around p clockwise and anticlockwise by an angle $\delta/2$, the boundary of C'' sweeps an area that contains D. For every point $q \in D$, since the distance between p and q is at most l by assumption, the distance between q and the boundary of C'' is at most $\delta l/2$, which implies that $q \in T$. Thus, $D \subset T$.

For all $r > 0$, the Minkowski sum of the boundary of C and a disk of radius r has area less than or equal to $2r \cdot \mathrm{peri}(C) + \pi r^2$, which implies that $|T| \leqslant \delta l \cdot \mathrm{peri}(C) + \pi\delta^2 l^2/4$. Since $\mathrm{peri}(C) \leqslant \pi \cdot \mathrm{diam}(C)$, we obtain $|D| \leqslant |T| \leqslant \pi\delta l \cdot \mathrm{diam}(C) + \pi\delta^2 l^2/4$. Hence, $|C \backslash C'| = \frac{1}{2}|D| \leqslant (\pi\delta l/2) \cdot \mathrm{diam}(C) + \pi\delta^2 l^2/8$. $\square$

The following lemma shows that two copies of a convex polyhedron have a small symmetric difference if the Hausdorff distance between them is small.

Lemma 6. *Let C be a convex polyhedron in $\mathbb{R}^3$. Let C' be a copy of C such that the Hausdorff distance between C and C' is at most l. Let c and b be the first and second largest principal diameters of $\mathcal{E}(C)$. Then $|C \backslash C'| \leqslant \pi l(b+2l)(c+2l)$.*

Proof. Every point $q \in C \backslash C'$ is at distance l or less from the boundary of C'. Denote the Minkowski sum of C' and a ball of radius l as $M_{C'}$. The volume of $C \backslash C'$ is at most the volume of $M_{C'} \backslash C'$. Then $|C \backslash C'|$ is at most l times the surface area of $M_{C'}$. Let E be an ellipsoid that is concentric with $\mathcal{E}(C')$ and has principal diameters $a+2l$, $b+2l$, and $c+2l$, where $a \leqslant b \leqslant c$ are the principal diameters of $\mathcal{E}(C')$. The ellipsoid E is the set of points at distance l or less from $\mathcal{E}(C')$. All points in $M_{C'}$ are at distance l or less from C'. It follows that $M_{C'} \subseteq E$ because $C' \subseteq \mathcal{E}(C')$. Therefore, for any plane H through the origin, the orthogonal projection of $M_{C'}$ in H is contained in the orthogonal projection of E in H. By the Cauchy's surface area formula [9], the surface area of a convex shape S in $\mathbb{R}^3$ is equal to the average area of the projection of S onto all possible planes through the origin. We conclude that the surface area of $M_{C'}$ is at most the surface area of E. Therefore, $|C \backslash C'|$ is at most l times the surface area of E, which is at most $\pi l(b+2l)(c+2l)$. □

The next result proves the correctness of our strategy to find a $(1-\varepsilon)$-approximately maximum overlap of P_1 and P_2 under rigid motion.

Lemma 7. *Let P_1 and P_2 be two convex polytopes in $\mathbb{R}^3$. Let ε be any value from $(0, 1/2]$. Suppose that the maximum overlap of P_1 and P_2 under rigid motion is at least $\lambda \cdot \max\{|P_1|, |P_2|\}$ for some constant $\lambda \in (0, 1]$. Then, there exists a rotation $\tilde{R}_* \in S_\beta \times S_\alpha \times S_\gamma$ and a translation $\tilde{T}$ such that $|\tilde{R}_\gamma(\tilde{R}_\beta(P_1)) \cap \tilde{T}(\tilde{R}_\alpha(P_2))|$ is at least $1-\varepsilon$ times the maximum overlap of P_1 and P_2 under rigid motion.*

Proof. The rotation part $\mathring{R}_*$ of the optimal rigid motion is represented by a triple of angles $(\mathring{\theta}_\beta, \mathring{\theta}_\alpha, \mathring{\theta}_\gamma) \in I_\beta \times I_\alpha \times I_\gamma$. For all $\xi \in \{\beta, \alpha, \gamma\}$, let $\tilde{\theta}_\xi$ be the closest value in S_ξ to $\mathring{\theta}_\xi$. Then, $(\tilde{\theta}_\beta, \tilde{\theta}_\alpha, \tilde{\theta}_\gamma)$ defines a rotation $\tilde{R}_*$. $\tilde{R}_\beta$, $\tilde{R}_\alpha$, and $\tilde{R}_\gamma$ are the rotations around the β_1-axis, the α_2-axis, and the $\tilde{R}_\beta(\gamma_1)$-axis that comprise $\tilde{R}_*$. Let $\tilde{T}$ denote the translation that maximizes the overlap of $\tilde{R}_\gamma(\tilde{R}_\beta(P_1))$ and $\tilde{R}_\alpha(P_2)$. Let $\mathring{T}$ denote the translation that maximizes the overlap of $\mathring{R}_\gamma(\mathring{R}_\beta(P_1))$ and $\mathring{R}_\alpha(P_2)$. Therefore,

$$\left|\tilde{R}_\gamma\left(\tilde{R}_\beta(P_1)\right) \cap \tilde{T}\left(\tilde{R}_\alpha(P_2)\right)\right| \geqslant \left|\tilde{R}_\gamma\left(\tilde{R}_\beta(P_1)\right) \cap \mathring{T}\left(\tilde{R}_\alpha(P_2)\right)\right|.$$

We analyze the difference between the maximum overlap and the approximate overlap as follows.

$$\begin{aligned}
&\left|\mathring{R}_\gamma\left(\mathring{R}_\beta(P_1)\right) \cap \mathring{T}\left(\mathring{R}_\alpha(P_2)\right)\right| - \left|\tilde{R}_\gamma\left(\tilde{R}_\beta(P_1)\right) \cap \tilde{T}\left(\tilde{R}_\alpha(P_2)\right)\right| \\
&\quad\leqslant \left|\mathring{R}_\gamma\left(\mathring{R}_\beta(P_1)\right) \cap \mathring{T}\left(\mathring{R}_\alpha(P_2)\right)\right| - \left|\tilde{R}_\gamma\left(\tilde{R}_\beta(P_1)\right) \cap \mathring{T}\left(\tilde{R}_\alpha(P_2)\right)\right| \\
&\quad= \left|\mathring{R}_\gamma\left(\mathring{R}_\beta(P_1)\right) \cap \mathring{R}_\alpha\left(\mathring{T}(P_2)\right)\right| - \left|\tilde{R}_\gamma\left(\tilde{R}_\beta(P_1)\right) \cap \tilde{R}_\alpha\left(\mathring{T}(P_2)\right)\right| \\
&\quad= \left|\mathring{R}_\gamma\left(\mathring{R}_\beta(P_1)\right) \cap \mathring{R}_\alpha\left(\mathring{T}(P_2)\right)\right| - \left|\tilde{R}_\gamma\left(\mathring{R}_\beta(P_1)\right) \cap \mathring{R}_\alpha\left(\mathring{T}(P_2)\right)\right| && (1) \\
&\qquad+ \left|\tilde{R}_\gamma\left(\mathring{R}_\beta(P_1)\right) \cap \mathring{R}_\alpha\left(\mathring{T}(P_2)\right)\right| - \left|\tilde{R}_\gamma\left(\mathring{R}_\beta(P_1)\right) \cap \tilde{R}_\alpha\left(\mathring{T}(P_2)\right)\right| && (2) \\
&\qquad+ \left|\tilde{R}_\gamma\left(\mathring{R}_\beta(P_1)\right) \cap \tilde{R}_\alpha\left(\mathring{T}(P_2)\right)\right| - \left|\tilde{R}_\gamma\left(\tilde{R}_\beta(P_1)\right) \cap \tilde{R}_\alpha\left(\mathring{T}(P_2)\right)\right|. && (3)
\end{aligned}$$

If a point p lies in $\mathring{R}_\gamma(\mathring{R}_\beta(P_1)) \cap \mathring{R}_\alpha(\mathring{T}(P_2))$ but not in $\tilde{R}_\gamma(\mathring{R}_\beta(P_1)) \cap \mathring{R}_\alpha(\mathring{T}(P_2))$, then $p \in \mathring{R}_\gamma(\mathring{R}_\beta(P_1))$ but $p \notin \tilde{R}_\gamma(\mathring{R}_\beta(P_1))$. The common rotation $\mathring{R}_\beta$ can be ignored. Thus,

$$\left|\mathring{R}_\gamma\left(\mathring{R}_\beta(P_1)\right) \cap \mathring{R}_\alpha\left(\mathring{T}(P_2)\right)\right| - \left|\tilde{R}_\gamma\left(\mathring{R}_\beta(P_1)\right) \cap \mathring{R}_\alpha\left(\mathring{T}(P_2)\right)\right| \leqslant \left|\mathring{R}_\gamma(P_1) \setminus \tilde{R}_\gamma(P_1)\right|.$$

Similar reasoning shows that

$$\begin{aligned}
&\left|\tilde{R}_\gamma\left(\mathring{R}_\beta(P_1)\right) \cap \mathring{R}_\alpha\left(\mathring{T}(P_2)\right)\right| - \left|\tilde{R}_\gamma\left(\mathring{R}_\beta(P_1)\right) \cap \tilde{R}_\alpha\left(\mathring{T}(P_2)\right)\right| \leqslant \left|\mathring{R}_\alpha(P_2) \setminus \tilde{R}_\alpha(P_2)\right|, \\
&\left|\tilde{R}_\gamma\left(\mathring{R}_\beta(P_1)\right) \cap \tilde{R}_\alpha\left(\mathring{T}(P_2)\right)\right| - \left|\tilde{R}_\gamma\left(\tilde{R}_\beta(P_1)\right) \cap \tilde{R}_\alpha\left(\mathring{T}(P_2)\right)\right| \leqslant \left|\tilde{R}_\gamma\left(\mathring{R}_\beta(P_1)\right) \setminus \tilde{R}_\gamma\left(\tilde{R}_\beta(P_1)\right)\right|.
\end{aligned}$$

Let H be a plane perpendicular to the γ_1-axis of P_1 that intersects $\mathring{R}_\gamma(P_1)$ and $\tilde{R}_\gamma(P_1)$. The convex polygon $H \cap \tilde{R}_\gamma(P_1)$ is rotated from the convex polygon $H \cap \mathring{R}_\gamma(P_1)$ by an angle at most $\varepsilon\Delta_\gamma$ around the point $\gamma_1 \cap H$. The diameter of $H \cap \tilde{R}_\gamma(P_1)$ is at most b_1. Since the rotation center $\gamma_1 \cap H$ is at distance $b_1/2$ or less from any point in $H \cap \mathring{R}_\gamma(P_1)$, Lemma 5 can be applied. Thus, $|(H \cap \mathring{R}_\gamma(P_1)) \setminus (H \cap \tilde{R}_\gamma(P_1))| \leqslant \pi\varepsilon b_1^2\Delta_\gamma/4 + \pi\varepsilon^2 b_1^2\Delta_\gamma^2/32$, which is less than $\pi\varepsilon b_1^2\Delta_\gamma/2$ because $\varepsilon\Delta_\gamma < 1$. Therefore,

$$\left|\mathring{R}_\gamma(P_1) \setminus \tilde{R}_\gamma(P_1)\right| \leqslant c_1 \cdot \frac{\pi}{2}\varepsilon b_1^2\Delta_\gamma = \frac{\pi}{2 \cdot 3^5}\varepsilon a_{\min} b_{\min} c_{\min}.$$

Similar reasoning shows that

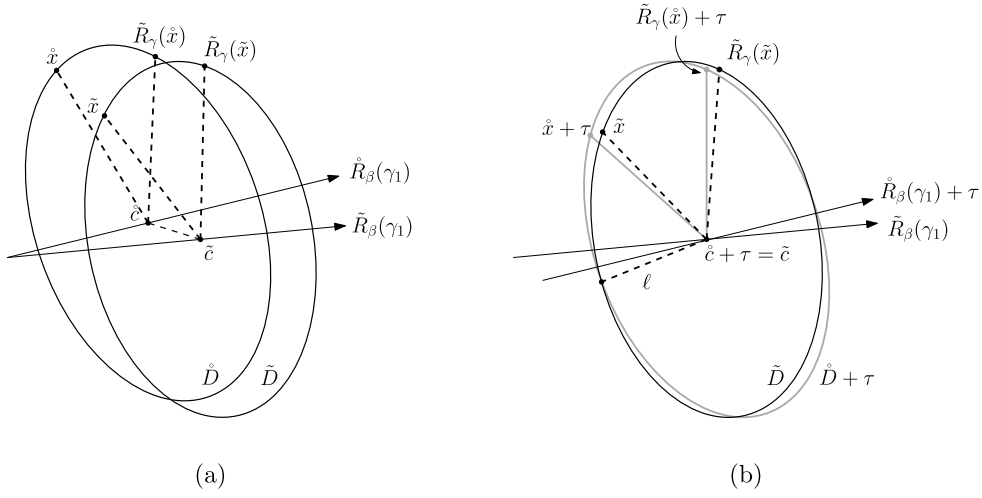

Fig. 3. Illustrations for bounding $\|\tilde{R}_\gamma(\mathring{R}_\beta(x)) - \tilde{R}_\gamma(\tilde{R}_\beta(x))\|$.

$$\left|\mathring{R}_\alpha(P_2) \setminus \tilde{R}_\alpha(P_2)\right| \leqslant a_2 \cdot \frac{\pi}{2}\varepsilon c_2^2 \Delta_\alpha = \frac{\pi}{2\cdot 3^5}\varepsilon a_{\min} b_{\min} c_{\min}.$$

Substituting the above results into (1)–(3) gives

$$\begin{aligned}&\left|\mathring{R}_\gamma\left(\mathring{R}_\beta(P_1)\right) \cap \mathring{T}\left(\mathring{R}_\alpha(P_2)\right)\right| - \left|\tilde{R}_\gamma\left(\tilde{R}_\beta(P_1)\right) \cap \tilde{T}\left(\tilde{R}_\alpha(P_2)\right)\right| \\ &\quad\leqslant \left|\tilde{R}_\gamma\left(\mathring{R}_\beta(P_1)\right) \setminus \tilde{R}_\gamma\left(\tilde{R}_\beta(P_1)\right)\right| + \frac{\pi}{3^5}\varepsilon a_{\min} b_{\min} c_{\min}. \end{aligned} \tag{4}$$

We bound $|\tilde{R}_\gamma(\mathring{R}_\beta(P_1)) \setminus \tilde{R}_\gamma(\tilde{R}_\beta(P_1))|$ as follows. $\tilde{R}_\gamma(\mathring{R}_\beta(P_1)) \setminus \tilde{R}_\gamma(\tilde{R}_\beta(P_1))$ may be non-empty because the angle between $\mathring{R}_\beta(\gamma_1)$ and $\tilde{R}_\beta(\gamma_1)$ can be as large as $\varepsilon\Delta_\beta/2$. This slight misalignment causes the results to be different after rotating $\mathring{R}_\beta(P_1)$ and $\tilde{R}_\beta(P_1)$ around $\mathring{R}_\beta(\gamma_1)$ and $\tilde{R}_\beta(\gamma_1)$, respectively, by the same angle $\tilde{\theta}_\gamma$.

Let x be a point of P_1. To apply Lemma 6, we need to bound the Hausdorff distance between $\tilde{R}_\gamma(\mathring{R}_\beta(x))$ and $\tilde{R}_\gamma(\tilde{R}_\beta(x))$. Let $\mathring{x} = \mathring{R}_\beta(x)$ and let $\tilde{x} = \tilde{R}_\beta(x)$. Let $\mathring{H}$ and $\tilde{H}$ be the planes that contain $\mathring{x}$ and $\tilde{x}$, respectively, and are orthogonal to $\mathring{R}_\beta(\gamma_1)$ and $\tilde{R}_\beta(\gamma_1)$, respectively. Let $\mathring{c}$ be the point $\mathring{H} \cap \mathring{R}_\beta(\gamma_1)$, and let $\tilde{c}$ be the point $\tilde{H} \cap \tilde{R}_\beta(\gamma_1)$. Note that $\|\mathring{c} - \tilde{c}\| \leqslant \varepsilon c_1 \Delta_\beta/2$ and $\|\mathring{c} - \mathring{x}\| = \|\tilde{c} - \tilde{x}\| \leqslant b_1/2$. $\tilde{R}_\gamma$ rotates $\mathring{x}$ on the boundary of a disk $\mathring{D} \subset \mathring{H}$ with center $\mathring{c}$ and radius $r = \|\mathring{c} - \mathring{x}\| \leqslant b_1/2$. Similarly, $\tilde{R}_\gamma$ rotates $\tilde{x}$ on the boundary of a disk $\tilde{D} \subset \tilde{H}$ with center $\tilde{c}$ and the same radius $r = \|\tilde{c} - \tilde{x}\| = \|\mathring{c} - \mathring{x}\|$. Fig. 3(a) shows an example.

We apply a translation $\tau = \tilde{c} - \mathring{c}$ to $\mathring{D}$. That is, τ translates $\mathring{D}$ to align $\mathring{c}$ with $\tilde{c}$. Fig. 3(b) shows the effect of τ. The intersection $\tilde{D} \cap (\mathring{D} + \tau)$ is a diameter of $\tilde{D}$. Let ℓ be a common radius of $\tilde{D}$ and $\mathring{D} + \tau$ that lies on $\tilde{D} \cap (\mathring{D} + \tau)$. Note that ℓ is parallel to the β_1-axis because we rotated P_1 around the β_1-axis at first and therefore $\tilde{D}$ and $\mathring{D}$ are parallel to the β_1-axis. For the same reason the angle between ℓ and the line connecting $\tilde{x}$ and $\tilde{c}$ is the same as the angle between ℓ and the line connecting $\mathring{x} + \tau$ and $\mathring{c} + \tau = \tilde{c}$. Since the same rotation $\tilde{R}_\gamma$ is applied to both $\mathring{R}_\beta(P_1)$ and $\tilde{R}_\beta(P_1)$, $\mathring{x}$ and $\tilde{x}$ are rotated on the boundary of $\mathring{D}$ and $\tilde{D}$ respectively with the same angle $\tilde{\theta}_\gamma$. Therefore the angle between ℓ and the line connecting $\tilde{R}_\gamma(\tilde{x})$ and $\tilde{c}$ is the same as the angle between ℓ and the line connecting $\tilde{R}_\gamma(\mathring{x}) + \tau$ and $\mathring{c} + \tau = \tilde{c}$. It follows that the acute angle between the line segment connecting $\tilde{c}$ and $\tilde{R}_\gamma(\tilde{x})$ and the line segment connecting $\mathring{c} + \tau$ and $\tilde{R}_\gamma(\mathring{x}) + \tau$ is no more than the angle between $\tilde{D}$ and $\mathring{D} + \tau$. The angle between $\mathring{D} + \tau$ and $\tilde{D}$ is same as the angle between $\mathring{R}_\beta(\gamma_1)$ and $\tilde{R}_\beta(\gamma_1)$, so $\|\tilde{R}_\gamma(\mathring{x}) + \tau - \tilde{R}_\gamma(\tilde{x})\| \leqslant \varepsilon r \Delta_\beta/2$.

By the triangle inequality,

$$\begin{aligned}\left\|\tilde{R}_\gamma\left(\mathring{R}_\beta(x)\right) - \tilde{R}_\gamma\left(\tilde{R}_\beta(x)\right)\right\| &\leqslant \|\mathring{c} - \tilde{c}\| + \left\|\tilde{R}_\gamma(\mathring{x}) + \tau - \tilde{R}_\gamma(\tilde{x})\right\| \\ &\leqslant \varepsilon c_1 \Delta_\beta + r\varepsilon\Delta_\beta/2 \\ &\leqslant 3\varepsilon c_1 \Delta_\beta/4.\end{aligned}$$

The above relation holds for every point $x \in P_1$, which means that the Hausdorff distance between $\tilde{R}_\gamma(\mathring{R}_\beta(P_1))$ and $\tilde{R}_\gamma(\tilde{R}_\beta(P_1))$ is at most $\varepsilon c_1 \Delta_\beta$. We apply Lemma 6 with $C = \tilde{R}_\gamma(\mathring{R}_\beta(P_1))$, $C' = \tilde{R}_\gamma(\tilde{R}_\beta(P_1))$, and $l = 3\varepsilon c_1 \Delta_\beta/4 \leqslant \varepsilon a_{\min} b_{\min} c_{\min}/(2^3 3^5 b_1 c_1)$. Therefore, Lemma 6 gives

$$\left|\tilde{R}_\gamma\left(\mathring{R}_\beta(P_1)\right) \setminus \tilde{R}_\gamma\left(\tilde{R}_\beta(P_1)\right)\right| \leqslant \pi l(b_1 + 2l)(c_1 + 2l)$$

$$\begin{aligned}
&\leqslant \pi b_1 c_1 l + 4\pi c_1 l^2 + 4\pi l^3 \\
&\leqslant \frac{\pi}{2^3 3^5}\varepsilon a_{\min} b_{\min} c_{\min} + \frac{\pi}{2^4 3^{10}}\varepsilon^2 a_{\min}^2 c_{\min} + \frac{\pi}{2^7 3^{15}}\varepsilon^3 a_{\min}^3 \\
&< \frac{\pi}{2^2 \cdot 3^5}\varepsilon a_{\min} b_{\min} c_{\min}.
\end{aligned}$$

Substituting this inequality into (4) shows that $|\mathring{R}_\gamma(\mathring{R}_\beta(P_1)) \cap \mathring{T}(\mathring{R}_\alpha(P_2))| - |\tilde{R}_\gamma(\tilde{R}_\beta(P_1)) \cap \tilde{T}(\tilde{R}_\alpha(P_2))| < 5\varepsilon\pi a_{\min} b_{\min} c_{\min}/(12 \cdot 3^4)$. Since $\frac{1}{3}\mathcal{E}(P_1) \cap \frac{1}{3}\mathcal{E}(P_2)$ lies inside $P_1 \cap P_2$ and has volume at least $\pi a_{\min} b_{\min} c_{\min}/(2 \cdot 3^4)$, it follows that $|\mathring{R}_\gamma(\mathring{R}_\beta(P_1)) \cap \mathring{T}(\mathring{R}_\alpha(P_2))| - |\tilde{R}_\gamma(\tilde{R}_\beta(P_1)) \cap \tilde{T}(\tilde{R}_\alpha(P_2))|$ is at most ε times the maximum overlap of P_1 and P_2 under rigid motion. □

4. Main algorithm

We use the result of the previous section to sample a set of rotations $S_\beta \times S_\alpha \times S_\gamma$ from $I_\beta \times I_\alpha \times I_\gamma$. For each rotation $R_* \in S_\beta \times S_\alpha \times S_\gamma$, we want to compute the best translation to align $R_\gamma(R_\beta(P_1))$ and $R_\alpha(P_2)$, and then keep track of the rigid motion $M = (T, R_*)$ encountered so far that gives the largest overlap. For efficiency purpose, we compute the "almost best" translation using Theorem 8 below. There is enough slack in the proof of Lemma 7 so that the analysis still works as long as we invoke Theorem 8 with $\mu < \pi\varepsilon a_{\min} b_{\min} c_{\min}/(12 \cdot 3^4)$. Algorithm 1 shows the pseudocode of our algorithm.

Theorem 8. *(See [3].) Let P_1 and P_2 be two convex polytopes in $\mathbb{R}^3$ specified by n bounding planes. For any fixed $\mu > 0$, we can compute an overlap of P_1 and P_2 under translation that is at most μ less than the optimum. The running time is $O(n \log^{3.5} n)$ with probability $1 - n^{-O(1)}$.*

Algorithm 1 Maximum overlap approximation algorithm.

```
1: procedure MaxOverlap(P1, P2, ε)                    ▷ return (1 − ε)-optimal rigid motion
2:     Compute E(P1) and E(P2) and align their centers and the respective axes.
3:     Compute three sets of sampled angles Sβ, Sα, and Sγ.
4:     ans := 0
5:     M := null
6:     for all rotation R* ∈ Sβ × Sα × Sγ do
7:         Compute the translation T to align Rγ(Rβ(P1)) and Rα(P2) using Theorem 8
8:         if |Rγ(Rβ(P1)) ∩ T(Rα(P2))| > ans then
9:             ans := |Rγ(Rβ(P1)) ∩ T(Rα(P2))|
10:            M := (R*, T)
11:        end if
12:    end for
13:    return M
14: end procedure
```

Theorem 9. *Let P_1 and P_2 be two convex polytopes in $\mathbb{R}^3$ specified by n bounding planes. Suppose that the maximum overlap of P_1 and P_2 under rigid motion is at least $\lambda \cdot \max\{|P_1|, |P_2|\}$ for some given constant $\lambda \in (0, 1]$. For all $\varepsilon \in (0, 1/2)$ and for all $n \geqslant 1/\varepsilon$, Algorithm 1 runs in $O(\varepsilon^{-3} n \log^{3.5} n)$ time with probability at least $1 - n^{-O(1)}$ and returns a $(1-\varepsilon)$-approximate maximum overlap of P_1 and P_2 under rigid motion.*

Proof. The approximation factor of Algorithm 1 is guaranteed by Lemma 7. We analyze its running time as follows. First, it takes $O(n)$ time to compute the ellipsoids $\mathcal{E}(P_1)$ and $\mathcal{E}(P_2)$ by Lemma 1. The remaining time spent by Algorithm 1 is $|S_\beta| \cdot |S_\alpha| \cdot |S_\gamma| \cdot n \log^{3.5} n$ with probability at least $1 - n^{-O(1)}$. Thus, it suffices to bound $|S_\beta| \cdot |S_\alpha| \cdot |S_\gamma|$, which is $O(\varepsilon^{-3} \cdot |I_\beta||I_\alpha||I_\gamma| \cdot (\Delta_\beta \Delta_\alpha \Delta_\gamma)^{-1})$.

Suppose that $2^{20} 3 a_{\min} > \lambda^2 c_{\min}/\sqrt{2}$. Then $I_\xi = (-\pi, \pi]$ for all $\xi \in \{\beta, \alpha, \gamma\}$. The assumption of $2^{20} 3 a_{\min} > \lambda^2 c_{\min}/\sqrt{2}$ implies that $a_{\min}$, $b_{\min}$, and $c_{\min}$ are within constant factors of each other. Therefore, $\Delta_\beta \Delta_\alpha \Delta_\gamma = \Theta(1)$ by Lemma 3, which implies that $|S_\beta| \cdot |S_\alpha| \cdot |S_\gamma| = O(\varepsilon^{-3})$. Thus, the running time is $O(\varepsilon^{-3} n \log^{3.5} n)$ with probability $1 - O(\varepsilon^{-3} n^{-O(1)}) = 1 - n^{-O(1)}$ because we assume that $n \geqslant 1/\varepsilon$.

Suppose that $2^{20} 3 a_{\min} \leqslant \lambda^2 c_{\min}/\sqrt{2}$. Then $|I_\beta| = O(a_{\min}/c_{\min})$ and, by Lemma 3, $\Delta_\beta = \Theta(a_{\min}/c_{\min})$. Therefore, $|I_\beta|/\Delta_\beta = O(1)$. By definition, $|I_\alpha| = O(b_{\min}/c_{\min})$ and, by Lemma 3, $\Delta_\alpha = \Theta(b_{\min}/c_{\min})$. Therefore, $|I_\alpha|/\Delta_\alpha = O(1)$. Similarly, $|I_\gamma| = O(a_{\min}/b_{\min})$ and, by Lemma 3, $\Delta_\gamma = \Theta(a_{\min}/b_{\min})$. Thus, $|I_\gamma|/\Delta_\gamma = O(1)$. We conclude that the running time in this case is also $O(\varepsilon^{-3} n \log^{3.5} n)$ with high probability. □

Acknowledgements

The authors would like to thank the anonymous reviewers for helpful comments.

References

[1] H.-K. Ahn, P. Brass, O. Cheong, H.-S. Na, C.-S. Shin, A. Vigneron, Inscribing an axially symmetric polygon and other approximation algorithms for planar convex sets, Computational Geometry: Theory and Applications 33 (2006) 152–164.

[2] H.-K. Ahn, P. Brass, C.-S. Shin, Maximum overlap and minimum convex hull of two convex polyhedra under translation, Computational Geometry: Theory and Applications 40 (2008) 171–177.

[3] H.-K. Ahn, S.-W. Cheng, I. Reinbacher, Maximum overlap of convex polytopes under translation, Computational Geometry: Theory and Applications 46 (2013) 552–565.

[4] H.-K. Ahn, O. Cheong, C.-D. Park, C.-S. Shin, A. Vigneron, Maximizing the overlap of two planar convex sets under rigid motions, Computational Geometry: Theory and Applications 37 (2007) 3–15.

[5] M. de Berg, O. Cheong, O. Devillers, M. van Kreveld, M. Teillaud, Computing the maximum overlap of two convex polygons under translations, Theory of Computing Systems 31 (1998) 613–628.

[6] S.-W. Cheng, C.-K. Lam, Shape matching under rigid motion, Computational Geometry: Theory and Applications 46 (2013) 591–603.

[7] O. Cheong, A. Efrat, Sariel Har-Peled, Finding a guard that sees most and a shop that sells most, Discrete & Computational Geometry 37 (2007) 545–563.

[8] H.J.A.M. Heijmans, A.V. Tuzikov, Similarity and symmetry measures for convex shapes using Minkowski addition, IEEE Transactions on Pattern Analysis and Machine Intelligence 20 (1998) 980–993.

[9] D.A. Klain, G.-C. Rota, Introduction to Geometric Probability, Cambridge University Press, 1997.

[10] F. Meyer, P. Bouthemy, Region-based tracking in an image sequence, in: Proceedings of the 2nd European Conference on Computer Vision, 1992, pp. 476–484.

[11] M.J. Todd, E.A. Yıldırım, On Khachiyan's algorithm for the computation of minimum volume enclosing ellipsoids, Discrete Applied Mathematics 155 (2007) 1731–1744.

[12] R.C. Veltkamp, M. Hagedoorn, State of the art in shape matching, in: M. Lew (Ed.), Principles of Visual Information Retrieval, Springer, 2001, pp. 87–119.

[13] A. Vigneron, Geometric optimization and sums of algebraic functions, in: Proceedings of the 21st Annual ACM–SIAM Symposium on Discrete Algorithms, 2010, pp. 906–917.